Catal Lett (2009) 127:392–399
DOI 10.1007/s10562-008-9706-z

Unusual Catalytic Performance for Selective Acetylene Hydrogenation over Pd Nanoparticles Fabricated on N,O-containing Organic Groups Modified Silica

Kangjun Wang · Yangying Chen · Xiaosong Li · Huixian Ding

Received: 10 October 2007 / Accepted: 8 January 2008 / Published online: 7 November 2008

Abstract A novel Pd-based catalyst, small Pd nanoparticles (1-2 nm) fabricated on N,O-containing organic groups modified silica, exhibits unusual catalytic performance for selective hydrogenation of acetylene, that is, the ethylene selectivity rises significantly with the increase of acetylene conversion regardless of the variation of reaction temperature or hydrogen partial pressure until 100% acetylene conversion. The in situ DRIFTS spectra of CO adsorption show that the organic groups presented on the silica affect the electronic property of the very small Pd nanoparticles.

Keywords Pd nanoparticles · Organic groups modified silica · Acetylene hydrogenation · Ethylene

1 Introduction

Selective hydrogenation of acetylene to ethylene is one of the important industrial processes and the Pd-based catalyst has been the one with the best performance for this reaction. Due to the poor selectivity at high acetylene conversion, especially at high H_2 partial pressure, remarkable research interests have been focusing on developing more selective catalysts. In the past decades, it has been found that, over the poorly dispersed Pd catalysts, multiple Pd sites and β-phase Pd-hydride can be formed, these two kinds of sites are detrimental to ethylene selectivity [1–3]. When improving the dispersion (decreasing particles size from 3 to 1 nm), however, the turnover frequency (TOF) of alkyne greatly decreased due to its strong adsorption on small electron-deficient clusters [4, 5], which also affected alkene selectivity [6, 7]. So far, it is generally recognized that the electronic and morphological properties of the Pd particles play a dominant role in its catalytic performance [8, 9]. Based on this account, several strategies for tuning the electronic and/or morphological properties of Pd-based catalyst by incorporating a second metal such as Au, Ag, Cu and alkali metals [7, 10–12], decorating Pd particles with Si [13], pre-treatment with oxygen-containing compounds [14, 15], modifying the supports with transition-metal oxides [16] or by selectively poisoning active Pd sites with CO [6, 17] have been used to improve their selectivity. Although some of these measures are effective to improve the selectivity of ethylene (S_E), to the best of our knowledge, the ethylene selectivity usually decreases with the increase of acetylene conversion, especially at nearly 100% acetylene conversion and the high molar ratio of H_2/C_2H_2.

It is well known that the method of catalyst preparation and the support properties significantly affect the size, electronic and/or morphological properties of the supported metal particles [9, 18, 19], which may have strong influence on its catalytic performance. Recently, the organically modified mesoporous materials, which can graft the metal complexes or stabilize the metal nanoparticles, have attracted extensive research in heterogeneous catalysis [20, 21]. Because the metal precursors can be highly dispersed on the support surface through strong interaction with the organic groups, after reduction, the metal nanoparticles highly dispersed on modified support have been achieved [22–26]. Amino groups on the support surface have been found to influence the catalytic performance of the supported catalyst [27], and the noble metal-polyamine catalysts also exhibited unusual catalytic performance [28].

K. Wang (✉) · Y. Chen · X. Li · H. Ding
Laboratory of Plasma Physical Chemistry, School of Chemical Engineering, Dalian University of Technology, Linggong Road, P.O. Box 288, Dalian 116024, China
e-mail: labplpc@dlut.edu.cn

Nevertheless, this kind of catalyst is mainly used in liquid phase reactions, as for gas phase reaction, limited progress [29] has been made up to now. Herein, we report for the first time that a novel Pd-based catalyst with small Pd particles (1–2 nm) on a N, O-containing organic groups modified silica shows unique catalytic performance for selective hydrogenation of acetylene, in which the S_E always rises with the increase of acetylene conversion regardless of increasing reaction temperature or hydrogen partial pressure in the range investigated.

2 Experimental

2.1 Catalyst Preparation and Characterization

Pd nanoparticles supported on N, O-containing organic groups modified silica (denoted as Pd/M–SiO_2) were prepared as following. Firstly, 2.0 mL tetraethoxylsilicate (TEOS) was added into the mixture of 5.0 mL aminopropyltriethoxysilane (APTES), 10 mL of aqueous ammonia solution (27 wt%) and 20 mL of deionized water. After stirring at room temperature for 30 h, the mixed solution was evaporated at 353 K and the obtained solid was further dried in air at 393 K for 12 h, leading to aminopropyl-functionalized silica (denoted as NH_2–SiO_2). After that, 1.0 g of NH_2–SiO_2 was added to 40 mL of aqueous solution of formaldehyde, and the mixture was stirred at 330 K for 5 h. The resulted suspension was filtered and washed with deionized water for several times and then fully dried under vacuum at 323 K for 5 h. The obtained white solid was denoted as $HOCH_2$–NH–SiO_2, on which the $HOCH_2HN$– groups were anchored, which had been demonstrated by Sun et al. [26]. To introduce Pd to the support, 1.0 g of $HOCH_2$–NH–SiO_2 was mixed with 40 mL of $PdCl_2$ aqueous solution (0.0012 M) and stirred at 330 K for 5 h. The obtained sample was washed with deionized water until no chlorine ions were detected in the filtrate and then dried under vacuum at 323 K for 5 h. The Pd catalyst thus prepared was denoted as I-Pd/M–SiO_2.

For comparison, a catalyst denoted as II-Pd/M–SiO_2 was prepared by tuning the pH value of $PdCl_2$ solution to 8-9 using aqueous ammonia solution before adding $HOCH_2$–NH–SiO_2 support, while other conditions was the same as the preparation of I-Pd/M–SiO_2 catalyst. Furthermore, the catalysts without organic groups were achieved by heating the I-Pd/M–SiO_2 catalyst at 673 K and 873 K in air, as denoted as I-Pd/M–SiO_2-673 and I-Pd/M–SiO_2-873, respectively. In addition, a similar loading of Pd supported on a commercial SiO_2 (Qingdao Haiyang Chemical Co., China), was prepared by using conventional incipient wetness impregnation [30]. In brief, after addition of the $PdCl_2$ solution to the silica, the mixture was dried at 383 K overnight, heated in air at 673 K for 3 h, and then kept in a desiccator (denoted as Pd/C–SiO_2). And in order to obtain the supported metallic Pd nanoparticles for reaction evaluation and characterization, each catalyst was reduced by H_2 stream at 473 K for 2 h unless stated otherwise.

The TEM images of the catalysts were recorded with transmission electron microscope (TEM, Philips Tecnai G^2 20). Pd loading was measured by ICP-AES (Optima 2000 DV). The N_2 adsorption isotherms at liquid nitrogen temperature were measured for the determination of BET surface area and porosity information, using the Micromeritics ASAP-2020 porosity analyzer. The XPS measurement was made on a Thermo spectrometer (VG ESCALAB250) equipped with a monochromatic Al $K\alpha$ (1486.6 eV) radiation source. To eliminate the effect of possible charge development in the sample during the XPS measurements, the observed peak position was calibrated using the C1 s peak (284.6 eV) as a reference. FTIR spectra of the catalyst samples and in situ DRIFTS spectra of CO adsorbed on the catalyst surface were determined using a Bruker TENSOR 27 IR spectrometer.

For in situ DRIFTS spectra of CO adsorption, the samples were firstly reduced at 473 K in H_2 for 2 h, and then switched to He for 0.5 h. After the temperature was decreased to 293 K in He, 20 mL/min of 2% CO in He was flowed through catalysts for 30 min, and then was switched to 40 mL/min of He for removing CO in gas, and the IR spectra was collected.

2.2 Reaction Testing

The selective acetylene hydrogenation was conducted in a quartz tube reactor (i.d. 4 mm) with total gas hourly space velocity (GHSV) of 80,000 mL h^{-1}(g cat.)$^{-1}$. The hydrocarbon concentration in the effluent gas from the reactor was analyzed by an on-line gas chromatography (Agilent 6890 N) equipped with a Porapak N column and a flame ionization detector. Steady-state conditions were maintained for 1 h for adequate sampling before varying the reaction temperature or H_2/C_2H_2 ratio to the next selected value. The S_E was defined as: S_E = ethylene formed/acetylene converted. All used gases are in high-purity grade (>99.99%).

3 Results and Discussion

3.1 TEM and XPS

The TEM images of I-Pd/M–SiO_2, I-Pd/M–SiO_2-673 and II-Pd/M–SiO_2 catalysts are displayed in Fig. 1. For I-Pd/M–SiO_2, it is clearly shown that highly dispersed palladium nanoparticles have been successfully fabricated on

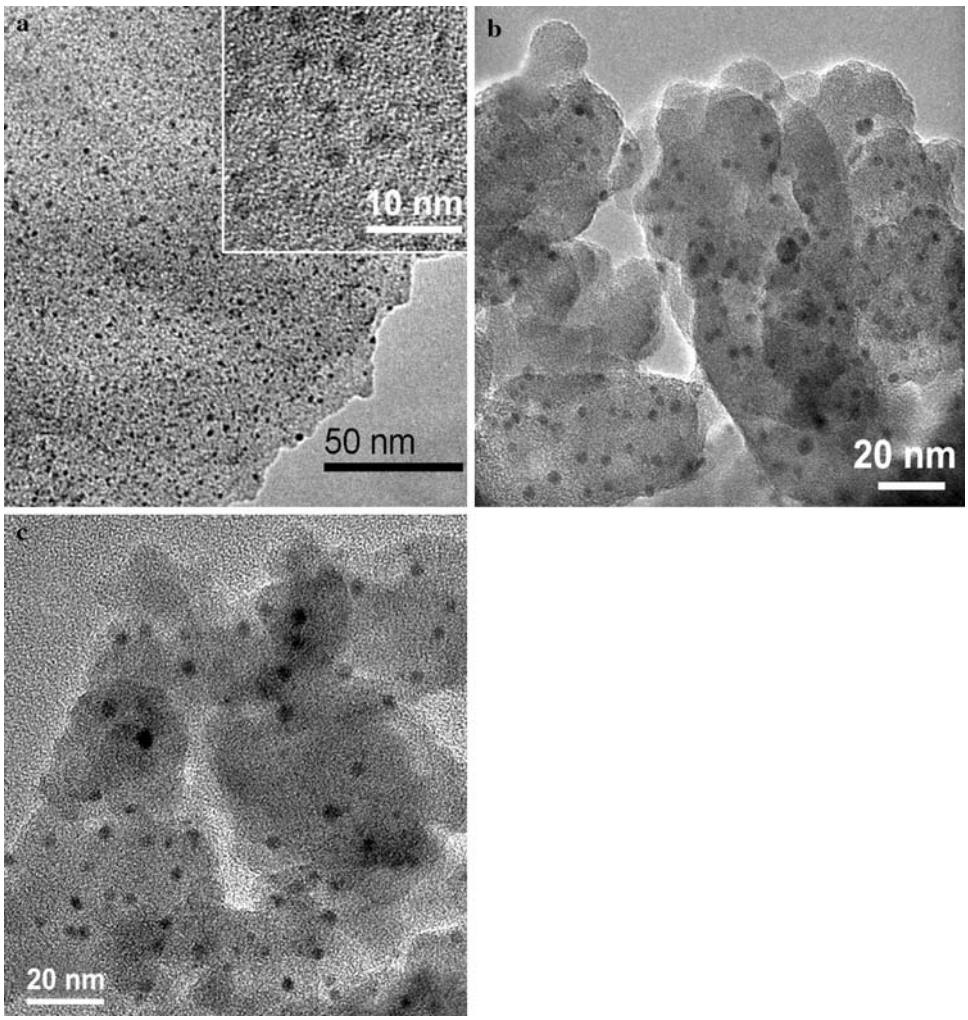

Fig. 1 TEM images of **a** I-Pd/M–SiO_2, **b** I-Pd/M–SiO_2-673 and **c** II-Pd/M–SiO_2

the hybrid organic-inorganic silica support in a nearly monodispersed fashion and narrow size distribution of 1-2 nm (Fig. 1a). Inevitably, the particle size of Pd increased to 2–4 nm when I-Pd/M–SiO_2 catalyst was calcined in air at 673 K (I-Pd/M–SiO_2-673), as shown in Fig. 1b. Figure 1c shows that the size of Pd nanoparticles of II-Pd/M–SiO_2 catalyst is as large as 2–4 nm, though a nearly monodispersion is also achieved in this case. It can be seen that the Pd particle size of II-Pd/M–SiO_2 is larger than that of I-Pd/M–SiO_2 catalyst. This may be due to the change of the ligands of precursors after addition of ammonia, that is, the Cl^- ion of the $[PdCl_4]^{2-}$ ions is displaced by NH_3 to form $[Pd(NH_3)_4]^{2+}$ ions. The $[Pd(NH_3)_4]^{2+}$ and $[PdCl_4]^{2-}$ions may anchor on the different reaction sites of the support, so the particle size changes.

XPS result of I-Pd/M–SiO_2 shows the binding energy of the Pd $3d_{5/2}$ level (334.9 eV) and Pd $3d_{3/2}$ level (340.3 eV), indicating exclusively metallic Pd particles with no significant amount of Pd oxidized species.

3.2 FTIR

Figure 2a shows the results of FTIR spectrum of NH_2–SiO_2. The appearance of the peaks at 3,358 cm^{-1}, 3,297 cm^{-1}, (assigned to N–H stretching), 1,600 cm^{-1} (assigned to scissoring in-plane bending mode of the primary amine NH_2 group) [31], 2,934 cm^{-1} and 2,880 cm^{-1} (assigning to the C–H of aminopropyl stretching) and the peaks between 1,700 and 1,300 cm^{-1} [32], clearly indicates that aminopropyl groups are introduced onto the silica via sol-gel condensation of TEOS and APTES. After further reaction with HCHO to form $HOCH_2$–NH–SiO_2, and introduction of Pd to yield Pd/M–SiO_2, the FTIR spectra of the two samples (Fig. 2b, c) show almost no strength change for the peaks associated with alkyl group despite the peaks related to amino groups are weakened, which proves that the organic groups are maintained during these processes. It can be seen that the organic groups are almost completely removed when I-Pd/M–SiO_2 catalyst is

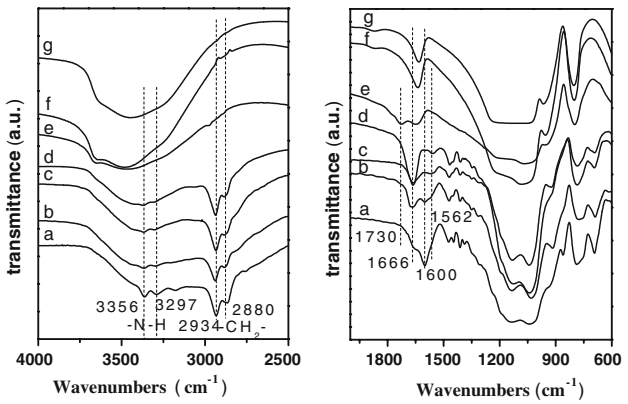

Fig. 2 FTIR spectra of **a** NH_2–SiO_2, **b** $HOCH_2$-NH–SiO_2, **c** I-Pd/M–SiO_2, **d** I-Pd/M–SiO_2 after reaction, **e** I-Pd/M–SiO_2-673, **f** I-Pd/M–SiO_2-873 and **g** Pd/C–SiO_2

calcined at 673 K and 873 K (Fig. 2e, f). The FTIR spectrum of I-Pd/M–SiO_2-873 is almost the same as that of Pd/C–SiO_2 (Fig. 2f, g), which distinctly demonstrates that the organic groups are removed.

3.3 BET

BET surface area and porosity information of the catalysts are presented in Table 1. It can be seen that I-Pd/M–SiO_2 and II-Pd/M–SiO_2 catalysts have similar BET surface areas (about 44 m^2/g) and average pore size (6 nm). After heating in air at 673 K, the BET of I-Pd/M–SiO_2 increased significantly, from 44 m^2/g to 432 m^2/g, and average pore size decreased from 6.6 nm to 2.6 nm for I-Pd/M–SiO_2-673 catalyst. The change of BET surface area may be caused by the organic component in the support. The BET surface area and average pore size of Pd/C–SiO_2 catalyst using commercial silica are 450 m^2/g (similar to that of I-Pd/M–SiO_2-673) and 6 nm (similar to that of I-Pd/M–SiO_2), respectively.

Table 1 BET surface area, pore volume and the average pore diameter of the catalysts

Sample	BET surface area (m^2/g)	Pore volume (cc/g)	Average pore diameter (nm)
I-Pd/M–SiO_2	44	0.080	6.6
II-Pd/M–SiO_2	43	0.082	6.7
I-Pd/M–SiO_2-673	432	0.28	2.6
Pd/C–SiO_2	450	0.66	6.0

3.4 Catalytic Performance for Selective Acetylene Hydrogenation

Figure 3 presents the effect of the reaction temperature on acetylene conversion and ethylene selectivity for selective acetylene hydrogenation over Pd-based catalysts. For Pd/C–SiO_2 catalyst, acetylene conversion increases with the increase of reaction temperature (curve a of Fig. 3a), and the S_E decreases dramatically with the increase of reaction temperature (curve a of Fig. 3b), which is in agreement with the literature results [7, 33–36]. However, for I-Pd/M–SiO_2 catalyst, it is striking that both the ethylene selectivity (from 24 to 68%, curve b of Fig. 3b) and acetylene conversion (from 16 to 100%, curve b of Fig. 3a) increase with the rising reaction temperature, which is drastically different from that of Pd/C–SiO_2 (curve a of Fig. 3b) and the results shown in literatures [7, 33–36]. Numerous previous work [2, 3, 6] have demontrated that the coke deposition can lead to the increase of ethylene selectivity. However, ethylene selectivity decreased with the decrease of acetylene conversion for I-Pd/M–SiO_2 catalyst when the reaction temperature decreased from 363 K to 300 K after the reaction was conducted from 300 K to 363 K. Thus the unusual results caused by coke may be ruled out. It is also not be ascribed to the effect of green oil, because which can lead to poor ethylene selectivity [3, 37].

In addition, the effect of H_2/C_2H_2 ratio on acetylene conversion and ethylene selectivity was also investigated over these catalysts (see Fig. 4). It shows that acetylene

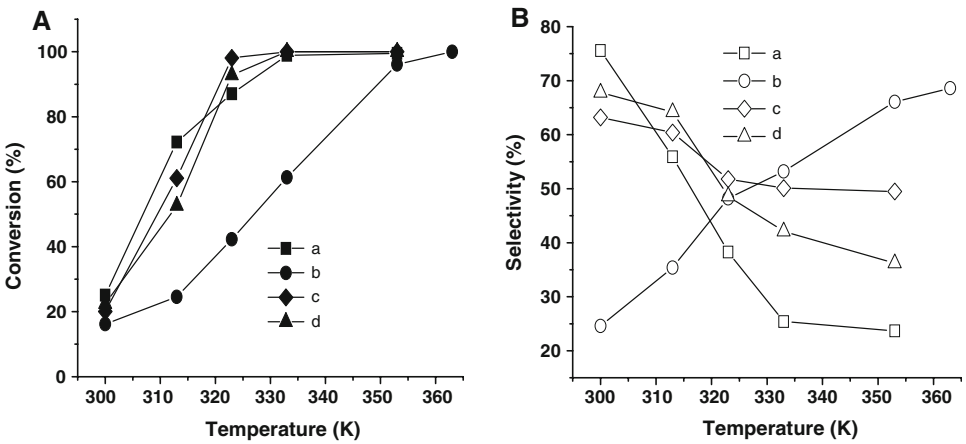

Fig. 3 Effect of temperature on **a** acetylene conversion and **b** ethylene selectivity over catalysts **a** 0.38 wt%Pd/C–SiO_2, **b** 0.42 wt% I-Pd/M–SiO_2, **c** 0.42 wt% I-Pd/M–SiO_2-673 K, and **d** 0.42 wt% I-Pd/M–SiO_2-873 K; H_2/C_2H_2 = 7/1, GHSV of 80,000 mL h^{-1}(g cat.)$^{-1}$

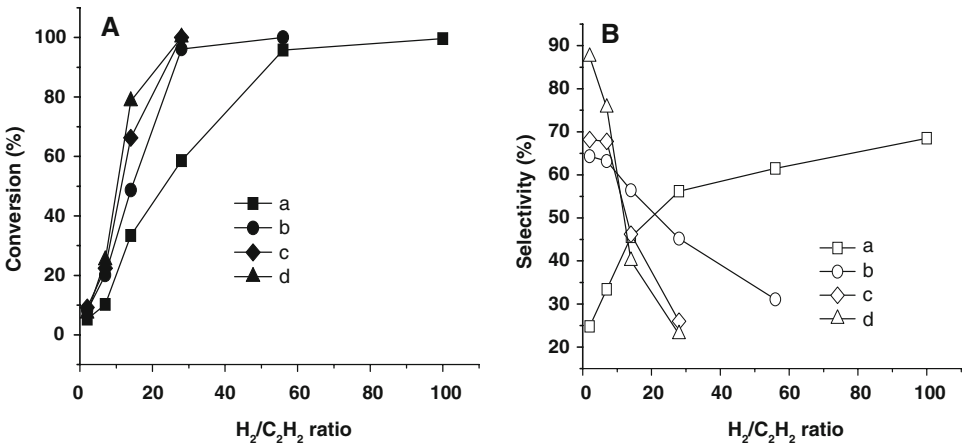

Fig. 4 Effect of H_2/C_2H_2 on **a** acetylene conversion and **b** ethylene selectivity over catalysts **a** 0.42 wt% I-Pd/M–SiO_2, **b** 0.42 wt% I-Pd/M–SiO_2-673, **c** 0.42 wt% I-Pd/M–SiO_2-873 and **d** 0.38 wt% Pd/C–SiO_2 under a GHSV of 80,000 mL h^{-1}(g cat.)$^{-1}$ at 300 K

conversion increases with the increase of the H_2/C_2H_2 ratio for all catalysts prepared here (Fig. 4a). In the case of ethylene selectivity, however, it is quite surprising that the ethylene selectivity increases remarkably with the increase of H_2/C_2H_2 ratio over I-Pd/M–SiO_2 catalyst (curve a of Fig. 4b). In contrast, ethylene selectivity decreases significantly for Pd/C–SiO_2, and calcined I-Pd/M–SiO_2 catalysts (I-Pd/M–SiO_2-673 and I-Pd/M–SiO_2-873), with the increase of H_2/C_2H_2 ratio (curve b-d of Fig. 4b), which is in line with the literature results [7, 38, 39]. To eliminate the unique phenomenon caused by coke, the experiment was conducted firstly at very high H_2/C_2H_2 ratio over I-Pd/M–SiO_2 catalyst, and then decreased to the low H_2/C_2H_2 ratio. The result showed that both acetylene conversion and ethylene selectivity decreased with the decrease of H_2/C_2H_2 ratio, which was almost the same as the result showed in curve a of Fig. 4a and curve a Fig. 4b (not shown here). In addition, previous work [2, 7] proposed that a high H_2/C_2H_2 ratio could drastically reduce the hydrocarbon coverage left irreversibly on the Pd sites due to the high hydrogen coverage. Thus high acetylene conversion was achieved, as well as the poor ethylene selectivity. Therefore it is less possible that the high ethylene selectivity was derived from the effect of coke at high H_2/C_2H_2 ratio.

The results over I-Pd/M–SiO_2 catalyst clearly indicate that the very low ethylene selectivity is obtained at low acetylene conversion, while the high ethylene selectivity is achieved at high acetylene conversion by increasing of reaction temperature or rising H_2/C_2H_2 ratio. It is well known that the adsorption capability of the acetylene is much stronger than the ethylene on the Pd catalyst [40], so the alkyne molecules can present on the surface of the catalyst in a high coverage ratio by displacing the alkene molecules from the surface of the catalyst or blocking their readsorption before all alkyne molecules are consumed virtually. In addition, the low H_2 pressure may favor the formation of small Pd sites due to deposition carbonaceous species on Pd surface, which permit the selective hydrogenation of acetylene but simultaneously inhibit the adsorption of ethylene [41]. Therefore, in normal case, high ethylene selectivity was obtained at low acetylene conversion and low H_2/C_2H_2 ratio. However, the results found on I-Pd/M–SiO_2 catalyst (Figs. 3 and 4) suggest that ethylene species formed from acetylene hydrogenation may not immediately remove from active sites by acetylene until total hydrogenation, because readsorption of ethylene is less possible in the presence of large amount of acetylene. With the increase of reaction temperature or by rising H_2/C_2H_2 ratio, the ethylene species may be easily removed from reaction site, the ethylene selectivity increases.

Based on the above results, we may conclude that the I-Pd/M–SiO_2 catalyst possesses the unique catalytic performance for selective hydrogenation of acetylene. As for the true origin of this unusual catalytic performance, the first reason may be considered is the effect of small Pd particles size. However, the size effect of Pd particle (even less than 1 nm) has been extensively investigated for selective alkyne hydrogenation over various conventional carriers during past years [4–6, 33, 42–44], the unique conversion-selectivity relationship presented here has never been reported. Thus it is less possible that the small Pd nanoparticles can cause the unusual catalytic performance for I-Pd/M–SiO_2 catalyst.

In contrast to Pd/C–SiO_2 and other catalysts found in the literatures, the I-Pd/M–SiO_2 catalyst contains organic groups, as confirmed by FTIR spectrum (Fig. 2c). It is worth noting that these organic groups are not removed during the acetylene hydrogenation reaction (Fig. 2d). It is well known that N-containing compound, as modifiers, which can efficiently affect the catalytic performance of the catalyst, have been extensively used in homogeneous and heterogeneous catalysis [45]. In order to investigate the effect of the organic composite, I-Pd/M–SiO_2 catalyst was calcined at 673 K and 873 K. The FTIR spectra show that the peaks attributed to organic groups almost completely disappeare after the calcination (Fig. 2e, f). The catalytic performance of the calcined catalysts (I-Pd/M–SiO_2-673

and I-Pd/M–SiO_2-873) is shown in Figs. 3 and 4. It can be seen that ethylene selectivity decreases with the increase of reaction temperature (curve c-d of Fig. 3b) or by rising H_2/C_2H_2 ratio (curve b-c of Fig. 4b) for the calcined catalysts, which is similar to that of Pd/C–SiO_2 catalyst and the results found in literatures, but completely different from that of I-Pd/M–SiO_2 catalyst, that is, the ethylene selectivity increases with the increase of reaction temperature or H_2/C_2H_2 ratio (Figs. 3a and 4a). In addition, the particle size inevitably increased during calcination (Fig. 1b), but just as mentioned above, the unique catalytic performance has never been observed only by reducing the Pd particles size [4–6, 33, 42–44]. Therefore, It suggests that the N,O-containing organic groups may play a crucial role for the unusual catalytic performance.

Do the organic groups always play this kind of role regardless of Pd particle size? To further clear it, compared tests with II-Pd/M–SiO_2 catalyst having larger particle size, 2–4 nm (as can be seen in Fig. 1c), was conducted under the simlar reaction conditions. The catalytic property of II-Pd/M–SiO_2 catalyst is shown in Fig. 5. It reveals that with the increase of acetylene conversion, ethylene selectivity increases slightly initially, but decreases after the acetylene conversion further reached up to 100% when the reaction temperature or H_2/C_2H_2 ratio rises continously. Obviously, the catalytic performance of II-Pd/M–SiO_2 catalyst is not as good as that of I-Pd/M–SiO_2 catalyst because of its larger Pd particle size (2–4 nm). This means that, even in the presence of organic groups, the catalyst with large Pd particles also can not lead to the unique catalytic performance. Therefore, it may be concluded that the unusual catalytic performance of I-Pd/M–SiO_2 may originate from the synergetic effect of the small Pd particles and its adjacent organic groups.

3.5 CO Chemisorption and In Situ DRIFTS

Figure 6 presents IR spectra relevant to the vibrational properties of adsorbed CO on different Pd-based catalysts, which can exhibit the structure and the charge properties of the supported Pd nanoparticles. For Pd/C–SiO_2 catalyst (Fig. 6a), two feature bands, 2,089 cm^{-1} and broad band 1,933–1,800 cm^{-1}, are observed, and they are assigned to the vibration of linear CO species and the bridge-bond and μ_3 hollow bond CO, respectively. For II-Pd/M–SiO_2 catalyst, the linear feature band of CO shifts down to 2,063 cm^{-1} (Fig. 6b), which are red-shifted by about 30 cm^{-1} with respect to Pd/C–SiO_2 catalyst, and about 15 cm^{-1} with respect to reference data for the similar Pd particle size (2–4 nm) [46]. In contrast, the linear feature band shifts down to 2,040 cm^{-1} for I-Pd/M–SiO_2 catalyst (Fig. 6c), which are red-shifted by about 50 cm^{-1} with respect to Pd/C–SiO_2 catalyst, and 30–40 cm^{-1} with respect to reference data for the similar Pd particle size (1–2 nm) [46]. Therefore, the red-shift derived from effect of the size-dependence can be rule out. Possible explanations may be due to the organic groups for the two catalysts. It has been reported that for ligand-capped Pt nanocrystal

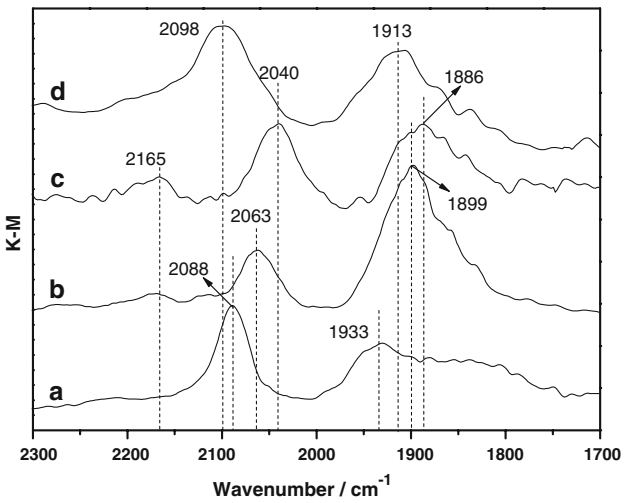

Fig. 6 IR spectra of CO adsorbed on various catalysts: **a** Pd/C–SiO_2, **b** II-Pd/M–SiO_2, **c** I-Pd/M–SiO_2, **d** I-Pd/M–SiO_2-673

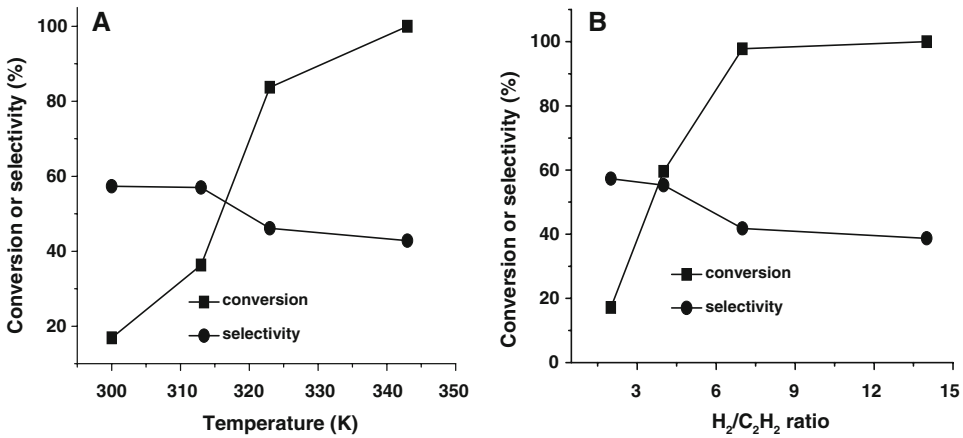

Fig. 5 The catalytic performance of 0.45 wt % II-Pd/M–SiO_2 catalyst: **a** Effect of reaction temperature on acetylene conversion and ethylene selectivity, $H_2/C_2H_2 = 2/1$, **b** Effect of H_2/C_2H_2 ratio on acetylene conversion and ethylene selectivity, 300 K of reaction temperature; GHSV of 80,000 mL h^{-1}(g cat.)$^{-1}$

(around 3 nm), 20–25 cm^{-1} red-shift was observed [47]. And it has been demonstrated that the very small metal nanoparticles can more effectively obtain the charge from organic ligands [48]. Here, compared with II-Pd/M–SiO_2, 20 cm^{-1} red-shift was also observed for I-Pd/M–SiO_2 catalyst (Fig. 6 b, c), which indicated that the small Pd particles of I-Pd/M–SiO_2 catalyst may also obtained more charge from organic groups. Figure 6d shows that the stretching frequencies of linear CO species significantly increase from 2,040 cm^{-1} to 2,098 cm^{-1} and the band at 1,886 cm^{-1} shifts up to 1,913 cm^{-1} when the organic groups are removed by calcination in air.

It is well known that the low back-donation of metal electrons into antibonding CO $2\pi^*$ will lead to the high values of υ(CO), but the low values of υ(CO) can be obtained when high back-donation of metal electrons into antibonding CO $2\pi^*$ [49]. In the present work, the high values of υ(CO), 2,089 cm^{-1} and 2,098 cm^{-1}, were obtained on Pd/C–SiO_2 and the calcined catalyst respectively, while the very low value of υ(CO), 2,040 cm^{-1}, was obtained over I-Pd/M–SiO_2 catalyst. These results clearly demonstrate that the electron density of small Pd clusters is dramatically influenced due to the presence of organic groups for I-Pd/M–SiO_2 catalyst. Nevertheless, the electronic property of Pd particles can strongly affect the absorption of reactant and the desorption of product, so the catalytic performance is changed. As for the details of the unique catalytic performance I-Pd/M–SiO_2 catalyst exhibited on acetylene hydrogenation, further work is under consideration.

Finally, the stability of I-Pd/M–SiO_2 catalyst was investigated, and it was found that the novel catalyst exhibits good stability and selectivity during 18 h at 363 K (Fig. 7).

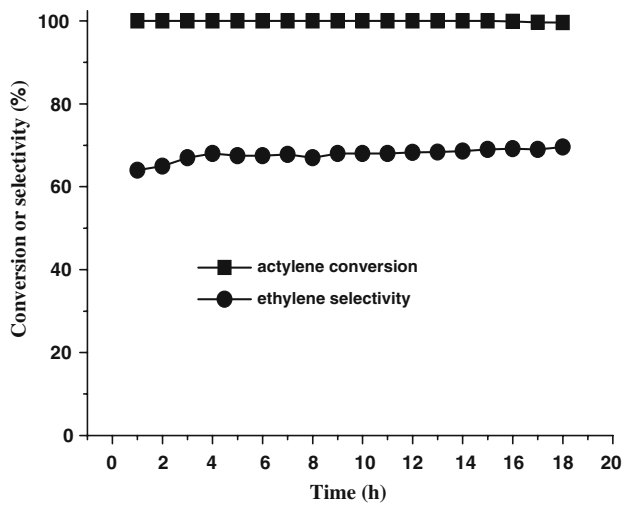

Fig. 7 Evaluation of acetylene conversion and ethylene selectivity as a function of time-on-stream over 0.42wt% I-Pd/M–SiO_2; H_2/C_2H_2 = 7/1, GHSV of 80,000 mL h^{-1}(g cat.)$^{-1}$, reaction temperature: 363 K

4 Conclusions

Highly dispersed Pd nanoparticles with uniform size distribution have been fabricated on the functionalized silica support by reducing the highly dispersed Pd precursor anchored on N,O-containing organic groups modified silica. The catalyst with a Pd particle size of 1-2 nm of I-Pd/M–SiO_2, exhibits unusual catalytic performance for selective acetylene hydrogenation in contrast to II-Pd/M–SiO_2 catalyst with larger Pd particle size (2–4 nm), Pd/C–SiO_2 and the calcined I-Pd/M–SiO_2 catalysts. With the using of I-Pd/M–SiO_2 catalyst, the ethylene selectivity rises significantly with the increase of acetylene conversion to 100% regardless of increasing reaction temperature or hydrogen partial pressure. While for other catalysts, ethylene selectivity decreases with the increase of reaction temperature or H_2/C_2H_2 ratio. It is proposed that the introduction of organic groups on the support may play a key role for the unique performance of I-Pd/M–SiO_2 catalyst through varying or tailoring the electronic structure of Pd nanoparticles with certain size (1–2 nm in present case), as the analysis of the IR spectra relevant to the vibrational properties of adsorbed CO. It is expected that the novel strategy may inspire researchers to explore new type of catalysts.

Acknowledgments This work was supported by Fok Ying Tung Education Foundation (Grant No. 94015), the National Natural Science Foundation of China (Grant Nos. 20106003, 20573014), and the Provincial Grants of Science and Technology of Liaoning, China (Grant No. 20032126).

References

1. Kang JH, Shin EW, Kim WJ, Park JD, Moon SH (2002) J Catal 208:310
2. Teschner D, Vass E, Hävecker M, Zafeiratos S, Schnörch HP, Sauer H, Gericke AK, Schlögl R, Chamam M, Wootsch A, Canning AS, Gamman JJ, Jacksonc SD, McGregor J, Gladden LF (2006) J Catal 242:26
3. Boradziński A, Bond GC (2006) Catal Rev 48:91
4. Ryndin YA, Nosova LV, Boronin AI, Chuvilin AL (1988) Appl Catal 42:131
5. Hub S, Hilaire L, Touroude R (1988) Appl Catal 36:307
6. Molnár Á, Sárkány A, Varga M (2001) J Mol Catal 173:185
7. Sárkány A, Horváth A, Beck A (2002) Appl Catal A 229:117
8. Narayanan R, El-Sayed MA (2005) J Phys Chem B 109:12663
9. Kalevaru VN, Benhmid A, Radnik J, Pohl MM, Bentrup U, Martin A (2007) J Catal 246:399
10. Huang DC, Chang KH, Pong WF, Tseng PK, Hung KJ, Hung WF (1998) Catal Lett 53:155
11. Leviness S, Nair V, Weiss AH, Schay Z, Guczi L (1984) J Mol Catal 25:131
12. Park YH, Price GL (1991) J Chem Soc Chem Commun 17:1188
13. Shin EW, Choi CH, Chang KS, Na YH, Moon SH (1998) Catal Today 44:137
14. Praserthdam P, Ngamsom B, Bogdanchikova N, Phatanasri S, Pramotthana M (2002) Appl Catal A 230:41

15. Panpranot J, Aungkapipattanachai S, Sangvanich T, Boonyaporn P, Praserthdam P (2007) React Kinet Catal Lett 91:195
16. Kang JH, Shin EW, Kim WJ, Park JD, Moon SH (2000) Catal Today 63:183
17. Butrihton GC, DalIon L, Tauvik GR (1982) Appl Catal 2:1
18. Arena F, Cum G, Gallo R, Parmaliana A (1996) J Mol Catal 110:235
19. Panpranot J, Kontapakdee K, Praserthdam P (2006) J Phys Chem B 110:8019
20. Song CE, Lee SG (2002) Chem Rev 102:3495
21. Vos DED, Dams M, Sels BF, Jacobs PA (2002) Chem Rev 102:3615
22. Chen YY, Qiu JS, Wang XK, Xiu JH (2006) J Catal 242:227
23. Gu JL, Shi JL, You GJ, Xiong LM, Qian SX, Hua ZL, Chen HR (2005) Adv Mater 17:557
24. Yang CM, Sheu HS, Chao KJ (2002) Adv Funct Mater 12:143
25. Yang CM, Liu PH, Ho YF, Chiu CY, Chao KJ (2003) Chem Mater 15:275
26. Sun JM, Ma D, Zhang H, Liu XM, Han XW, Bao XH, Weinberg G, Pfänder N, Su DS (2006) J Am Chem Soc 128:15756
27. Cao Y, Hu JC, Yang P, Dai WL, Fan KN (2003) Chem Commun 908
28. Macdonald RP, Winterbottm JM (1979) J Catal 57:195
29. Cao W, Zhang HB, Yuan YZ (2003) Catal Lett 91:243
30. Liu QS, Lunsford JH (2006) Appl Catal A: Gen 314:94
31. Ramanathan T, Fisher FT, Ruoff RS, Brinson LC (2005) Chem Mater 17:1290
32. Kasahara T, Inumaru K, Yamanaka S (2004) Micropor Mesopor Mater 76:123
33. AdÚriz HR, Bodnariuk P, Dennehy M, Gigola CE (1990) Appl Catal 58:227
34. Panpranot J, Nakkararuang L, Nagmsom B, Praserthdam P (2005) Catal Lett 103:53
35. Shi CK, Hoisington R, Jang BW-L (2007) Ind Eng Chem Res 46:4390
36. Shi CK, Jang BW-L (2006) Ind Eng Chem Res 45:5879
37. Sárkány A, Guczi L, Weiss AH (1984) Appl Catal 10:369
38. Bond GC, Wells PB (1965) J Catal 4:211
39. Moyes RB, Walker DW, Wells PB, Whan DA (1989) Appl Catal 55:5
40. Tysoe WT, Nyberg GL, Lambert RM (1983) J Chem Soc Chem Commun 11:623
41. Borodzinski A, Golebiowski A (1997) Langmuir 13:883
42. Sárkány A, Weiss AH, Guczi L (1986) J Catal 98:550
43. Gigola CE, Aduriz HR, Bodnariuk P (1986) Appl Catal 27:133
44. Ryndin YA, Stenin MV, Boronin AI, Bukhtiyarov VI, Zaikovskii VI (1989) Appl Catal 54:277
45. Mallat T, Baiker A (2000) Appl Catal A: Gen 200:3
46. Lear T, Marshall R, Lopez-Sanchez JA, Jackson SD, Klapötke TM, Bäumer M, Rupprechter G, Freund H-J, Lennon D (2005) J Chem Phys 123:174706
47. Borchert H, Fenske D, Kolny-Olesiak J, Parisi J, Al-Shamery K, Bäumer M (2007) Angew Chem Int Ed 46:2923
48. Qiu LM, Liu F, Zhao LZ, Yang WS, Yao JN (2006) Langmuir 22:4480
49. Fielicke A, von Helden G, Meijer G, Pedersen DB, Simard B, Rayner DM (2006) J Chem Phys 124:194305